Gas Processing Journal

Vol. 9, No. 1, 2021, pp. 29-42
http://gpj.ui.ac.ir

Research Paper

Energy and Environmental Comparison of Different Scenarios for Cogeneration of Power and Desalinated Water in Iran

Mohammad Javad Rahimi[1*], Homayun Alibabaee [2]

[1] National Center for Climate Change, Department of Environment of Islamic Republic of Iran (DOE), Tehran, Iran

[2] Faculty of Mechanical Engineering, Isfahan university of technology, Isfahan, Iran

Received: 2020-06-30 Revised: 2020-10-12 Accepted: 2020-10-18

Abstract: This paper presents a combined thermodynamic, economic, and environmental comparison of different configurations for co-production of power and desalinated water. Each configuration is analyzed both with inlet air cooling and without inlet air cooling. The most eminent characteristics for the comparison are cost of produced power, cost of produced water, total annual profit, CO_2 emission, and CHP efficiency. The common portions of all configurations are the gas turbine and the desalination system. The primary distinctions between scenarios are arrangement and type of system components. Thermodynamic simulation determines mass flow rate of high pressure and low pressure steam, as well as net power and water production of each configuration. Economic simulation reveals the price of produced power, the price of produced water and the total annual profit of the plant. Also, Environmental analysis specifies the total CO_2 emission per annum. Final results show that the third configuration, in which a double-pressure HRSG is utilized, has the lowest CO_2 emission per MWh of produced electricity. Also, it is concluded that the second configuration, in which a single-pressure HRSG is utilized, has the lowest specific fuel consumption and consequently the highest CHP efficiency. Sensitivity analysis shows that increasing the inlet air temperature will increase the specific CO_2 emission in the second configuration. On the other hand, inlet air temperature increase has a marginal impact on CO_2 emission in the first and the third configurations. The economic analysis shows that the first scenario with inlet air cooling has the highest total annual profit.

keywords: Thermodynamic and economic comparison, Environmental analysis, Desalination, Power and water cost, net annual profit

Graphical Abstract:

* different configurations for co-production of power and desalinated water analyzed.

* The impact of inlet air cooling on energy and environmental characteristics of the systems is evaluated.

* Environmental analysis specifies the total CO2 emission per annum for each configuration.

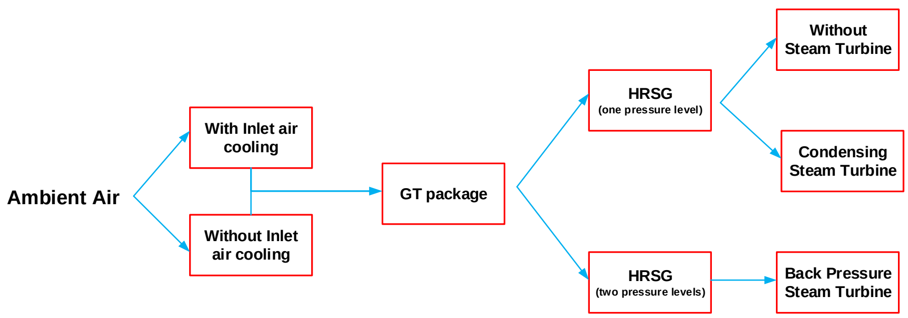

* Corresponding Author.
Authors' Email Address: [1] M.J. Rahimi (mohamad_rah@yahoo.com), [2] H. Alibabaee (h.alibabaee@gmail.com),

DOI: http:// 10.22108/gpj.2020.124627.1088

Nomenclature

CC	Combustion chamber
Comp	Compressor
C_p	Specific heat capacity at constant pressure
dea	Dearator
$\bar{h}$	Molar enthalpy
h	Enthalpy
HP	High pressure
HRSG	Heat Recovery Steam Generator
K	Ratio of the specific heat at constant pressure to the specific heat at constant volume
LP	Low pressure
$\dot{m}$	Mass flow rate
M	Mass flow rate (in desalination system analysis only)
MED	Multiple Effect Distillation
MSF	Multiple Stage Flash
n	The number of recovery and rejection stages of MSF system
O&M	Operation and Maintenance
P	Pressure
PSP	Power Sale Price
$\dot{Q}$	Time rate of heat
T	Temperature
TBT	Top Brine Temperature
TTD	Terminal Temperature Difference
WSP	Water Sale Price
subscripts	
a	air
av	average
b	brine
cw	Cooling water
d	distillate
f	feed
f	Fuel
i	Stage of desalination system
p	product
st	Steam turbine
Greek	
η_{it}	Isentropic efficiency of turbine
η_{ic}	Isentropic efficiency of compressor
η_{mt}	Mechanical efficiency of turbine
η_{mc}	Mechanical efficiency of compressor

1. Introduction

1.1. Literature review

Co-generation of desalinated water and electricity in southern areas of Iran which suffer from lack of enough freshwater sources is critical in attaining sustainable development targets. As a result, efforts have been made to utilize the desalination systems to produce fresh water from seawater. On the other hand, there are several gas turbine power plants in the southern region which produce large amounts of exhaust gases with relatively high temperature. So, there is a great opportunity for integrating the existing gas turbine power plants with thermal desalination systems for covering parts of the freshwater demands of southern cities of the country. As in the wintertime, the total natural gas consumption of the country increases considerably, the total efficiency of these systems is of great importance [1].

Thermal desalination is one of the most useful applications of cogeneration. Two major types of thermal desalination systems include MED and MSF. Different combinations of desalination systems have been studied in the literature [2, 3]. Desalination systems, in general, can be operated using low-grade heat from fossil fuel plants or renewable energy systems [4-6]. Different renewable energy systems may be incorporated into thermal systems for desalinated water production, including biomass combustion [7], a combination of solar and geothermal [8], and biomass gasification [9]. In our previous work, an analysis of multi-generation system fed by combined natural gas and synthesis gas (produced in a biomass gasification reactor) was performed [10].

Table 1 summarizes the recent research works, regarding the combined production of electricity and desalinated water with the use of fossil fuels.

Table 1: research works regarding the combined generation of freshwater and electricity

No.	Author(s)	Year	Main characteristics of the research
1.	Khoshgoftar et al. [2]	2020	* Energy and exergy analyses of Qom combined-cycle power plant coupled with a desalination system * it is concluded that the freshwater generation utilizing MED is significantly higher than MSF
2.	Manesh et al. [3]	2019	* combined exergetic and environmental analysis of coupling MSF, MED, and RO to a combined cycle power plant
3.	Sayyaddi et al. [11]	2018	Stirling- based desalination systems analyzed * generated 23.3 m^3/day of freshwater and 2.58 kW electricity
4.	Salimi et al. [12]	2017	* RO and MED desalination integration * R-curve concept utilized
5.	Sadri et al. [13]	2017	* Hybrid MED and RO desalination system taking into account the thermodynamic losses * optimization with the use of Genetic Algorithm
6.	Mokhtari et al. [14]	2016	* an integrated system, including gas turbine, MED, and RO * a reduction in final water price from 2.8 $/$m^3$ to 2.3 $/$m^3$ obtained
7.	Almutairi et al. [15]	2016	* combined production of electrical power and water using real data * reducing ambient temperature and increasing feed water temperature for enhancing the plant's performance
8.	Wu et al. [16]	2014	* development of a superstructure model to find optimal structure for variable demands of electricity, water, and heat
9.	Shakib et al. [17]	2012	* optimization of a cogeneration system coupled to MED desalination * considering HRSG design consideration in the optimization scheme
10.	Ansari et al. [18]	2014	* thermodynamic and economic analysis and optimization of a 1000 MW nuclear power plant coupled to MED–TVC
11.	Ameri et al. [19]	2009	* analysis of the impacts of inlet steam pressure, number of effects, and effects temperature difference on desalination system performance and specifications
12.	Kamali et al. [20]	2008	* parametric optimization of MED-TVC system to increase the gain output ratio of the system * using ODE for the modeling of transient nature of the temperature
13.	Nisan and Dardour [21]	2007	*water and power cost estimation in cogeneration plants consisting of nuclear reactors * two categories of desalination systems (MED and RO) coupled together
14.	Agashichev and El-Nashar [22]	2005	* predicting climate change and environmental impacts of electricity and freshwater generation * calculating CO_2 emission of a combined RO, MSF, and electricity generation block considered.
15.	Al-Hengari [23]	2005	* evaluation of design factors and operating conditions utilizing real data
16.	Alasfour et al. [24]	2005	* evaluation of different configurations of a MED-TVC * finding the impact of motive steam pressure, temperature, and flow rate on performance
17.	Kahraman and Cengel [25]	2005	* using actual data to analyze large MSF distillation plant * second law efficiency of the plant was 4.2%.

1.2. knowledge contribution and novelties

The major novelties of this paper are as follows:

- Simultaneous thermodynamic, economic, and environmental analysis of three different configurations for co-production of electricity and freshwater
- Introducing a novel evaluation methodology for comparing combined cycles of power, cooling, and water production based on the aggregate effects of economic and thermodynamic characteristics.
- Determination of the impact of inlet air cooling on the CO_2 emission of different configurations of heat recovery steam generator linked to the gas turbine package and desalination system.

Using the proposed configuration, both electricity and water demands of an area could be covered with higher efficiency. So, the proposed system can help in reaching a more sustainable future.

2. Process description and system configuration

As it will be shown in the figures, all configurations are similar in having a gas turbine which is a Siemens V94.2 (with a nominal power output of 148.8 MW in 15°C inlet air temperature) and the desalination system which is chosen to be MSF (Multi-Stage Flash) system, but the type of steam turbine and HRSG and consequently the way the desalination system is fed differs from case to case.

Furthermore, each configuration is analyzed in two different conditions: with inlet air cooling and without inlet air cooling.

2.1. Scenario 1

In this scenario (Fig. 1), the cycle is primarily composed of a Siemens v94.2 gas turbine, a one pressure HRSG, a backpressure steam turbine, a Multi-Stage Flash (MSF) desalination system for producing desalinated water, and a chiller for providing chilled water for inlet air cooling (If required).

As the steam turbine is backpressure type, the exiting steam of the steam turbine with required pressure is directed to brine heater as motive steam to heat the seawater. The heated seawater then goes to the first stage of the MSF system. Part of the heated seawater is flashed due to the low pressure of this stage relative to the vapor pressure of the heated brine. The flashed water is collected after condensing on the outer surface of the tube bundle of that stage.

The inputs of this scenario in two conditions, with inlet air cooling and without inlet air cooling, are presented in the table2:

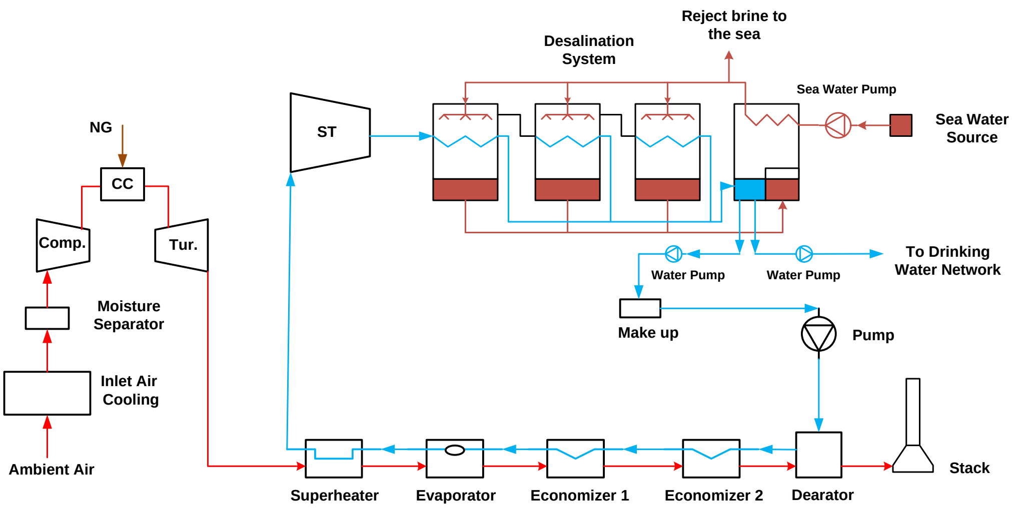

Fig. 1 The schematic diagram of the cycle of scenario 1

Table 2: input parameters of scenario 1

Input parameters	Without inlet air cooling	With inlet air cooling	Unit
Motive steam temperature to MSF	120.2	120.2	°C
Motive steam temperature to MSF	2	2	°C
Ambient air temperature (design)	35	35	°C
Inlet air temperature to compressor	35	10	°C
HRSG outlet steam temperature	510	510	°C
HRSG outlet steam pressure	86.8	86.8	Bar
Pinch temperature of evaporator	20	20	°C
Approach temperature of evaporator	5	5	°C
Top Brine Temperature (TBT)	110	110	°C
Terminal Temperature Difference (TTD)	7.5	7.5	°C

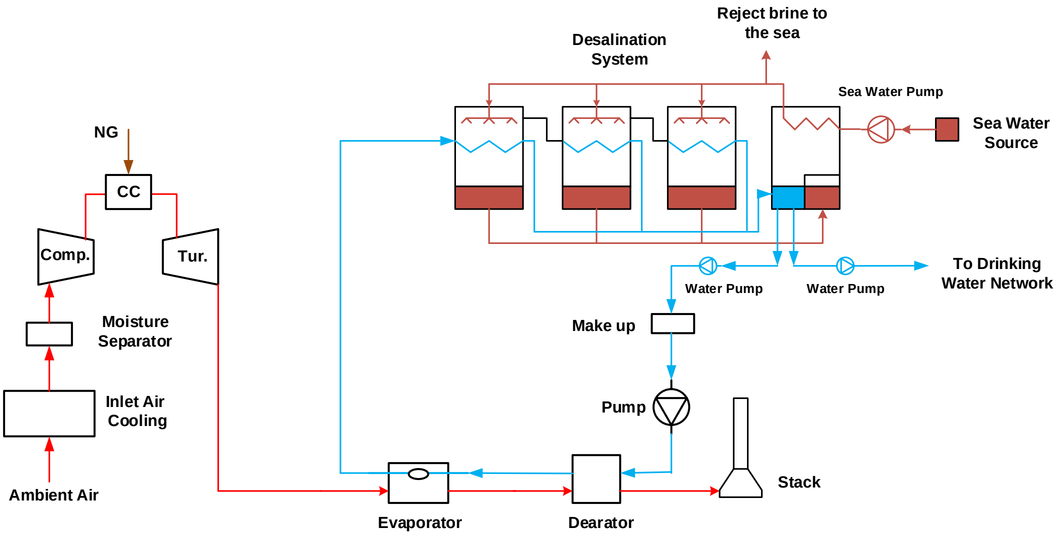

Fig. 2 The schematic diagram of the cycle of scenario 2

Table 3: input parameters of scenario 2

Input parameters	Without inlet air cooling	With inlet air cooling	Unit
Motive steam temperature to MSF	120.2	120.2	°C
Motive steam pres. to MSF	2	2	°C
Ambient air temperature (design)	35	10	°C
Inlet air temperature to compressor	35	10	°C
HRSG outlet steam temperature	122	510	°C
HRSG outlet steam pressure	2.14	86.8	Bar
Pinch temperature of evaporator	20	20	°C
Approach temperature of evaporator	5	5	°C
Top Brine Temperature (TBT)	110	110	°C
Terminal Temperature Difference (TTD)	7.5	7.5	°C

2.2. Scenario 2

As can be seen in Fig. 2, there is no steam turbine in this scenario, and the steam produced in the one pressure HRSG is directly used in the brine heater of the MSF system. The motive steam has a pressure of 2bar and a temperature of 121^c. The steam leaves the brine heater with a temperature of 117.5^c and in a saturated condition. The produced condensate returns to HRSG through the feed pump. The input data of this scenario is shown in table 3.

2.3. Scenario 3

In this case, two pressured HRSG is utilized. All the produced low-pressure steam plus a percent of low-pressure steam which is extracted from low-pressure stages of steam turbine, are mixed and directed to the brine heater, to increase the brine temperature and act as motive steam. The superheated steam generated in a high-pressure section of HRSG is utilized for power generation. Fig. 3 shows the schematic diagram of this configuration. Extraction of a portion of steam will decrease the steam turbines' power output; on the other hand, it increases the produced desalinated water. The presence of a condenser is indispensable in this configuration. The HRSG is comprised of three economizers, two evaporators, one deaerator, and one superheater with an industry acceptable configuration. Table 4 shows the major inputs of this configuration.

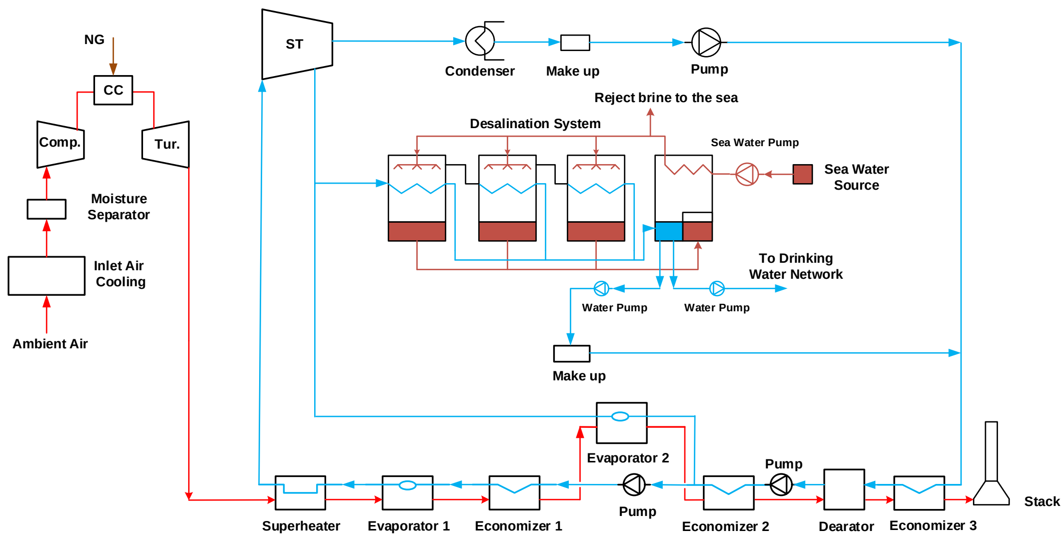

Fig. 3 The schematic diagram of the cycle of scenario 3

Table 4: input parameters of scenario 3

Input parameters	Without inlet air cooling	With inlet air cooling	Unit
Motive steam temperature to MSF	120	120	°C
Motive steam pressure to MSF	2	2	Bar
Ambient air temperature (design)	35	10	°C
Inlet air temperature to compressor	35	35	°C
HP steam temperature	510	510	°C
HP steam pressure	86.8	86.8	Bar
LP steam temperature	122	122	°C
LP steam pressure	2.14	2.14	Bar
Pinch temperature of 1st evaporator	20	20	°C
Pinch temperature of 2nd evaporator	20	20	°C
Approach temperature of 1st evaporator	5	5	°C
Approach temperature of 2nd evaporator	5	5	°C
Outlet temperature of economizer 3	104	104	°C
Top Brine Temperature (TBT)	110	110	°C
Terminal Temperature Difference (TTD)	7.5	7.5	°C

3. Simulation

3.1. Thermodynamic Simulation

Thermodynamic, economic, and environmental simulation of the three configurations are described in this section. The first step is to determine both the inputs and the outputs of the simulation.

The inputs include changeable decision variables and system parameters which are fixed during the simulation. The outputs are calculated from inputs, which are the fundamental laws of thermodynamics.

The major assumptions for simulation are shown in table 5. Siemens V94.2 gas turbine is selected for all three configurations and the ambient air temperature is considered 35 °C.

Other required inputs that are necessary for simulation include HP and LP steam pressure and temperature as well as the pinch and approach point temperature of heat recovery steam generator.

Dependent variables that are the desired outputs of the configurations are calculated based on the decision variables and simulation parameters. Major dependent variables are:

1- Power produced by the gas turbine
2- The gross power generation
3- The net power generation
4- The natural gas (input fuel) flow rate
5- Freshwater production flow
6- Total capital investment
7- Period of return
8- The net annual profit
9- CO_2 emission

Table 5: Major assumptions in all the three configurations

Name of parameter	value	unit
Ambient temperature	35	°C
Ambient relative humidity	75	%
air composition		
N_2-Ar	75.95	%
CO_2	0.03	%
H_2O	3.88	%
O_2	20.14	%
Inlet air temperature to compressor	changeable	°C
Superheater pressure drop (water side)	3.5	%
Economizer pressure drop (water side)	3	%
Steam turbine isentropic efficiency	85	%
Steam turbine mechanical efficiency	95.8	%
Water pumps isentropic efficiency	75	%
Water pumps mechanical efficiency	97	%
MSF number of stages (heat recovery)	18	
MSF number of stages (heat regenerative)	3	
Temperature of seawater	30	°C
Salinity of seawater	3.44	%

3.1.1. Gas Turbine Simulation

The gas turbine simulation is conducted through the thermodynamics laws, namely the first and the second laws of thermodynamics. Isentropic efficiency as well as mechanical efficiency concepts are employed in the simulation. It is assumed that the streams' physical properties are calculated in mean temperature and both combustion products and ambient air act as an ideal gas. The gas turbine schematic diagram is displayed in Fig. 4. The complete formulation for gas turbine modeling can be found in [26].

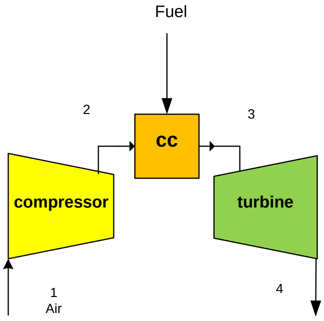

Fig. 4 The schematic diagram of the gas turbine

After analyzing the gas turbine and finding the mass flow rate, the composition, and the temperature of the leaving flue gas, the next stage is to calculate the characteristics of the water streams (i.e. the enthalpy and the entropy). For this purpose, it is necessary to determine the pressure and temperature of the waterside.

3.1.2. HRSG simulation

Finding the generated steam flow rate and water and gas temperature of all involved streams is the goal of HRSG simulation. For this purpose, it is necessary to do the pressure analysis of the gas and waterside of the system.

According to the assumptions of pressure drop in different parts of HRSG and with the use of the known pressures of the cycle, the pressure of every single stream can be found. The waterside pressure drop of the economizer is considered 3% of inlet pressure. Also, the waterside pressure drop of the superheater is considered 3.5% of inlet pressure. No pressure drop is considered for the waterside of the evaporator as it works in a saturated condition. The gas side pressure drop is assumed 2 mbar for each part of the HRSG.

3.1.3. Power calculation procedure

To calculate the output power of the steam turbine or the input power of water pumps, it is necessary to know flow rates, the enthalpies, and the mechanical efficiencies of the steam turbine and water pumps. The flow rates and the enthalpies are calculated according to the procedure mentioned in 3.1.2. The mechanical efficiencies are considered fixed as was mentioned in table 5.

3.2. Economic modeling

The major goal of the economic simulation is to determine the produced power and freshwater cost. It is also necessary to calculate the total annual profit of each configuration as one of the aims of the economic simulation. Power and freshwater costs are dependent on the net power and water output, O&M costs, fuel cost, etc. Since each configuration has its characteristics, its power and freshwater costs are different. Table 6 shows the major assumptions for economic simulation.

Table 6: Major economic data

Parameter	Symbol - unit	Value
Interest rate	i	0.15
Working years	n	15
Capital Recovery Factor	CRF	0.171
Working hours (per annum)	h	8117
availability	ava	0.926
Fuel Low heating value	LHV(kJ/kg)	50046.7
Price of fuel	$/GJ	3
Sale price (electricity)	$/kWh	0.05
Sale price (fresh water)	$/m³	1.111

3.2.1. Electrical power cost

The cost of produced electricity is composed of four terms, which stem from capital investment, fixed O&M cost, variable O&M cost, and fuel cost.

Capital investment includes the cost of all the major pieces of equipment of the system as well as all the minor costs. Furthermore, structural and civil works, piping work, equipment erection, wiring and electrical as well as the startup and engineering should be taken into account The electricity cost related to capital investment is determined through equation 1 below:

$$\cos t_{capital} = \frac{CAP \times 10^6 \times \mathrm{CRF}}{P \times 365 \times 24000 \times av} \quad (1)$$

"CAP" is the total investment (10^6 $) which is extracted from Thermoflow software [27], "CRF" is the capital recovery factor which is calculated according to equation 2, "n" is operation years, "i" is the rate of interest, "P" is the net electricity output (MW), and "av" is the availability of the plant.

$$CRF = \frac{i(1+i)^n}{(1+i)^n - 1} \quad (2)$$

Fixed O&M cost ranges from 10 to 40 $/kW-year. for the three above-mentioned configurations, 20 $/kW-year is considered [27].

Variable O&M cost which is usually expressed in $/kWh. For a co-generation plant, a reasonable value is 0.002 $/kWh as per the currently working plants of Iran.

Considering the price of the fuel which is assumed 0.003 $/(MJ LHV) and using equation 3, fuel cost can be calculated

$$cost_{fuel} = 0.003 \times HR \quad (3)$$

HR is the Heat Rate (MJ/kWh) and is calculated by equation 4:

$$HR = \frac{0.0036 \times \dot{m} \times LHV}{P} \quad (4)$$

$\dot{m}$ is the fuel flow rate (kg/s) and LHV is the fuel low heating value (kJ/kg).

3.2.2. Freshwater cost

The freshwater cost is composed of three parts which stem from capital investment, fixed O&M cost, and variable O&M cost ($/m^3.)

Capital investment is composed of transfer pumps, brine heat exchanger, stages, and related electrical, civil and structural, and piping works.

Equation 5 is utilized to calculate freshwater costs.

$$\cos t_{capital\_d} = \frac{capital\_d \times \varnothing \times 10^6}{V \times 4500 \times 365 \times avai} \quad (5)$$

The fixed and variable O&M costs of the desalination plant, are assumed 0.1159 $/m^3 and 0.0783 $/m^3 respectively. The total cost of freshwater production is the summation of the three above-mentioned terms.

3.3. Results of thermodynamic and economic modeling

The final results of thermodynamic and economic simulation of the first configuration are displayed in table 7.

As can be seen from Table 7, the total cost of produced power is 0.0286 $/kWh and the total cost of produced water is 0.7408 $/m^3. Also, the total annual profit which comes from selling power and water to the market is 35.103 M$ and the CHP efficiency is 67.08.

In table 8, a precise comparison between the three configurations for the combined production of power and desalinated power mentioned above is shown. CHP efficiency, Total annual profit, and the total cost of produced power and water are among the comparison parameters. For every configuration, two conditions are presented. The first one is the condition in which no inlet air cooling is applied (i.e. the inlet air temperature is 35 °C) and the second one is the condition that incorporates inlet air cooling for power augmentation (i.e. the inlet air temperature is 15 °C).

Table 8 shows that configuration 1 with inlet air cooling, has the highest total annual profit whereas configuration 2 with inlet air cooling, in which the steam produced in the one pressure HRSG is directly used in the brine heater, brings the highest CHP efficiency. The cost of electricity generation is the highest in configuration 3 with inlet air cooling (which is 0.0317 $/kWh) while the corresponding cost is lowest in configuration 2 with inlet air cooling (which is 0.0257 $/kWh). The cost of produced water is almost independent of inlet air cooling. The highest price of freshwater generation occurs in configuration 3 and the lowest occurs in configuration 2.

Table 7: thermodynamic and economic results of the first configuration (15 °C inlet air temp.)

name	unit	value
Net gas turbine Power output	MW	148.778
Net increased power output due to inlet air cooling	MW	14.461
Net steam turbine Power output	MW	44.042
Net total power output	MW	172.497
Desalinated water produced per day	MIGD	9.33
Fuel mass flow rate	kg/s	8.999
Net heat rate	MJ/kWh	5.366
Specialized equipment cost	M$	44.658
Other equipment cost	M$	2.584
Civil works cost	M$	2.86
Mechanical works cost	M$	6.681
Electrical and wiring works cost	M$	2.373
Structural works cost	M$	2.85
Startup and engineering cost	M$	4.476
Total capital cost of power generation	M$	66.482
Power cost due to the capital investment	$/kWh	0.0081
Fixed O&M cost	$/kW-year	20
Power cost due to Fixed O&M	$/kWh	0.0024
Variable O&M cost	$/kWh	0.002
Power cost due to variable O&M	$/kWh	0.002
Fuel price	$/MJ	0.003
Power cost due to the consumed fuel	$/kWh	0.0161
Total cost of produced power	$/kWh	0.0287
Total capital investment of MSF system	M$	45.387
Water cost due to the capital investment	$/m^3	0.5466
Water cost due to Fixed O&M	$/m^3	0.1159
Water cost due to variable O&M	$/m^3	0.0783
Total cost of produced water	$/m^3	0.7409
Annual profit	M$	35.103
CHP efficiency	%	67.084

Table 8: the comparison between thermodynamic and economic performance of all three configurations

	Total net power output	Total capital cost of power generation	Total cost of produced power	Total water production	Total capital cost of water generation	Total cost of produced water	CHP efficiency	Total annual profit
units	MW	M$	$/kWh	MIGD	M$	$/m^3	%	M$
Configuration 1 (without inlet air cooling)	158.036	60.311	0.0275	9.355	45.526	0.7410	71.69	34.04
Configuration 1 (with inlet air cooling)	172.497	66.482	0.0286	9.33	45.387	0.7408	67.08	35.10
Configuration 2 (without inlet air cooling)	106.343	46.112	0.0271	15.64	69.969	0.6969	79.89	29.61
Configuration 2 (with inlet air cooling)	124.527	51.957	0.0257	15.98	69.969	0.6862	86.34	34.83
Configuration 3 (without inlet air cooling)	176.714	70.818	0.0306	5	24.818	0.7519	60.95	30.52
Configuration 3 (with inlet air cooling)	192.081	78.192	0.0317	5	24.818	0.7519	57.82	31.24

3.3.1. Impact of the GT inlet air temperature on CO_2 emission

The Impact of changing inlet air cooling on the value CO_2 emission per MW of generated electricity is displayed in Fig. 5. In configuration 2, the inlet air temperature increases will increase the CO_2 emission too. On the other hand, the rate of CO_2 increase is marginal in configuration 1 and almost negligible in configuration 3. In fact, in configuration 2, increasing the air inlet temperature from 5 to 30 will increase the CO_2 emission from 599.05 kg/MWh to 632.41 kg/MWh which is a 5.5% increase.

The reasoning is that in configuration and 3; the rate of decrease of electricity generation (as a result of inlet air temperature increase) is almost identical to the rate of decrease in natural gas consumption and consequently the exhaust flue gas mas flow rate. But in configuration 2, the rate of decrease of electricity generation (as a result of inlet air temperature increase) is higher than the rate of decrease in the exhaust flue gas mass flow rate which is mainly due to the system arrangement.

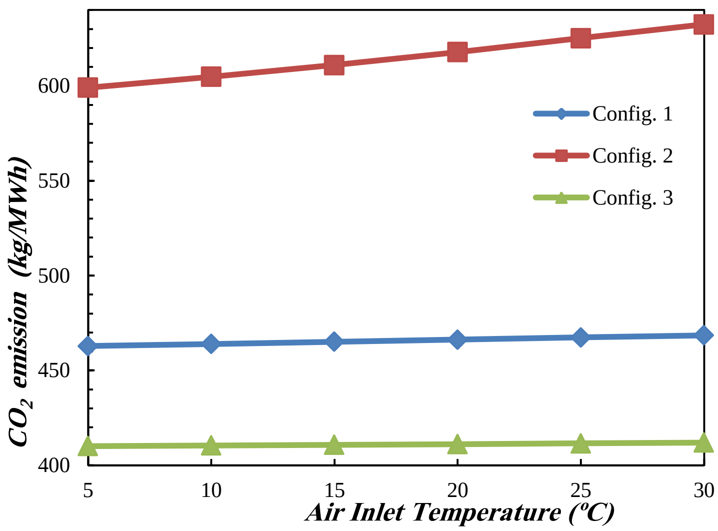

Fig. 5 Carbon Dioxide emission as a function of GT inlet air temperature

3.3.2. Impact of the GT inlet air temperature on desalinated water production

The impact of inlet air temperature on total desalinated water generation can be seen in Fig. 6.

As can be observed, as the inlet air temperature increases, three different trends are observable depending on the configuration. For the first configuration, a marginal increase in freshwater generation (from 488.2 kg/s to 492.6 kg/s) occurs. For the second configuration, a decrease in freshwater generation from 855.2 kg/s to 829.1 kg/s occurs and in the third configuration, no change occurs due to the change in inlet air temperature.

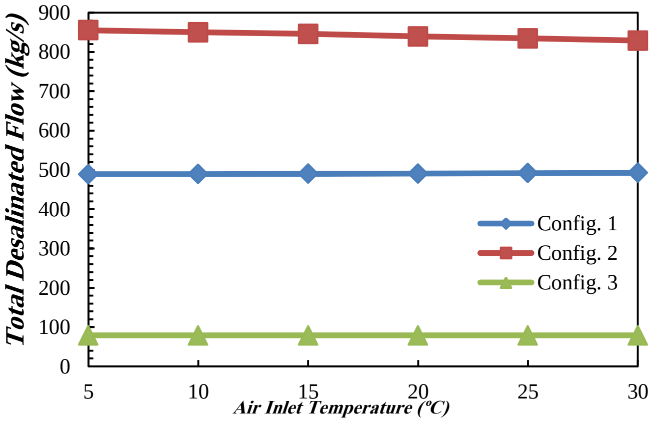

Fig. 6 Total desalinated flow as a function of GT inlet air temperature

3.3.3. Impact of the GT inlet air temperature on gross electrical output

By changing the inlet air temperature from 5 °C to 30 °C the gross electric power decreases with the same trend in all three configurations. In configuration 3, the gross power decreases from 198.57 MW to 175.57 MW. Similarly, in configuration 2, the gross power decreases from 153.43 MW to 130.08 MW. Finally, in configuration 3, a decrease from 224.12 MW to 199.87 MW can be observed.

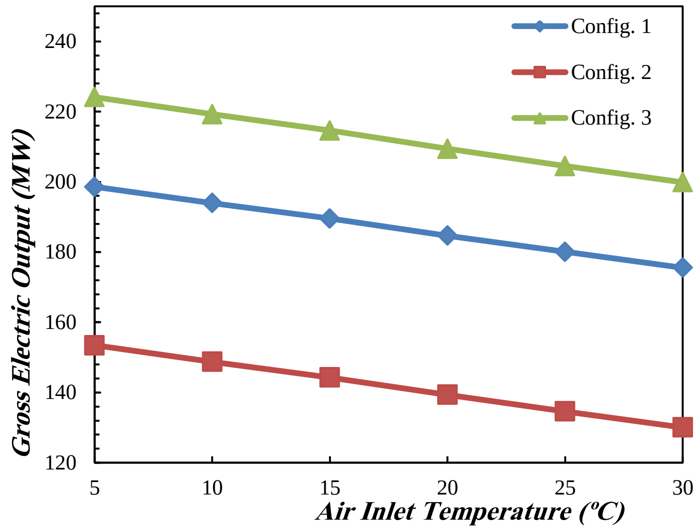

Fig. 7 Gross electric output as a function of GT inlet air temperature

3.3.4. Impact of the GT inlet air temperature on net electricity generation output

Similar to the trend of change of gross electricity generation due to the inlet air temperature, the net electricity generation decreases as the inlet air temperature increases from 5 °C to 30 °C. The course of change is shown in Fig. 8 below. Fig. 8 shows the rate of change of net electricity generation, due to the change of inlet air temperature is gentler than the rate of change of gross electricity generation. It is also observable that the rate of change of net power generation due to the inlet air temperature variation is not linear in all of the three configurations.

For example, in configuration 1, the maximum rate of power generation change occurs between 10 °C and 25 °C. Generally speaking, the minimum change rate occurs between 5 °C and 10 °C in all the configurations.

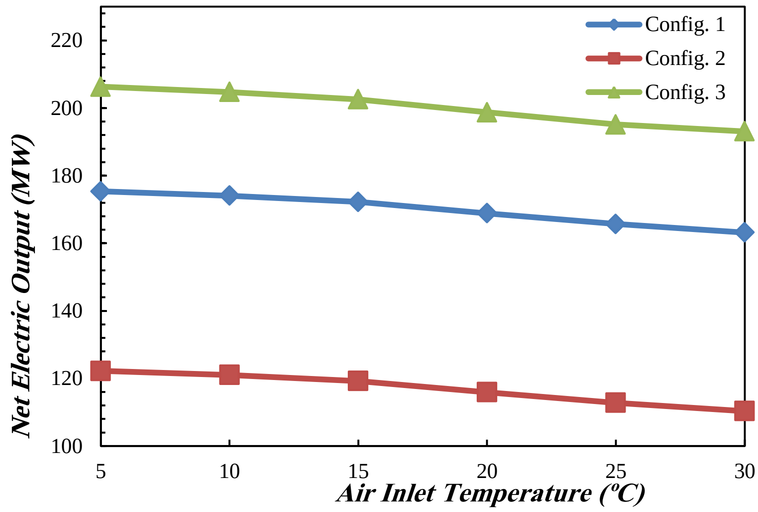

Fig. 8 Net electrical output as a function of GT inlet air temperature

3.3.5. Impact of the GT inlet air temperature on gross electrical efficiency

The impact of changing gas turbine inlet air temperature on gross electrical efficiency is demonstrated in Fig. 9 below. As it is displayed, the gross electric efficiency is independent of inlet air temperature in configuration 3. On the other hand, in configuration 2, the gross electric efficiency decreases as the inlet air temperature increases. Finally, in configuration 1, a marginal decrease in gross electric efficiency can be observed as the inlet air temperature increases, the efficiency decreases from 43.17% to 42.64%.

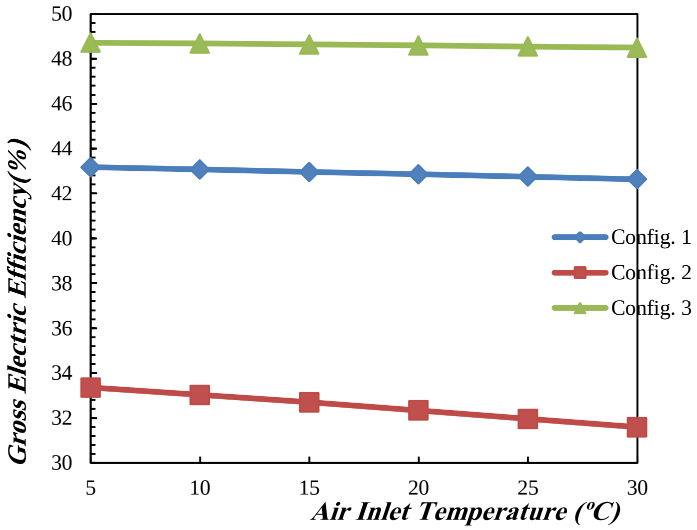

Fig. 9 Gross electrical efficiency as a function GT inlet air temperature

3.3.6 Impact of the GT inlet air temperature on net electrical efficiency

Fig. 10 demonstrates the effect of inlet air temperature on net electrical efficiency. Contrary to the trend of gross electrical efficiency which was discussed above, the net electrical efficiency increases as the inlet air temperature increases. It is observed that as a result of increasing inlet air temperature from 5 ºC to 30 ºC, the efficiency increases from 38.12% to 39.64%. It is also observed that the rate of increase is quite the same for configuration3. In configuration 2, a marginal increase from 26.57% to 26.88% occurs as the temperature increases from 5 ºC to 10 ºC but no further increase occurs as the temperature increases from 10 ºC to 30 ºC.

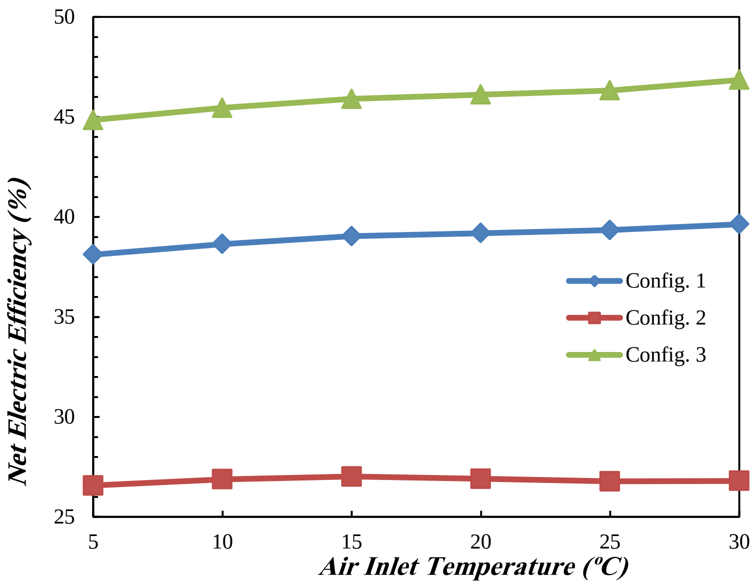

Fig. 10 Net electrical efficiency as a function GT inlet air temperature

4. Conclusion

In this paper, three combined productions of power and desalinated water were modeled, analyzed, and compared from thermodynamic, environmental, and economic points of view. The impact of inlet air cooling on the thermodynamic and economic performance of each configuration was investigated. The most important outputs of the modeling were the gross and net power output, CO_2 emission, total desalinated water produced, electrical and CHP efficiency, total power cost, total water cost, and finally net annual profit. The results of modeling showed that the first scenario with inlet air cooling had the highest total annual profit. On the other hand, the second scenario with inlet air cooling had the highest CHP efficiency. Evaluation of the impact of the amount of inlet air cooling on CO_2 emission, desalinated water production, electricity generation, and electrical efficiency was done in the last section. As the heart of electricity generation of all configurations is a V94.2 gas turbine and this mark of the gas turbine is the most common type of gas turbine in Iran, in those areas, where seawater is available or the quality of well or surface waters is inappropriate, the proposed configurations may be utilized.

References

[1] Rahimi MJ, Hamedi MH, Amidpour M. Thermodynamic, Economic and Case Study of Synthesis Gas Using the Biomass Gasification Reactor in Distributed Generation Systems. mdrsjrns. 2019;19:1417-28.

[2] Khoshgoftar Manesh MH, Kabiri S, Yazdi M, Petrakopoulou F. Thermodynamic evaluation of a combined-cycle power plant with MSF and MED desalination. Journal of Water Reuse and Desalination. 2020;10:146-57.

[3] Manesh MHK, Kabiri S, Yazdi M. Exergoenvironmental analysis and evaluation of coupling MSF, MED and RO desalination plants with a combined cycle plant. International Journal of Exergy. 2020;33:76-97.

[4] Ghorbani B, Ebrahimi A, Moradi M, Ziabasharhagh M. Energy, exergy and sensitivity analyses of a novel hybrid structure for generation of Bio-Liquefied natural Gas, desalinated water and power using solar photovoltaic and geothermal source. Energy Conversion and Management. 2020;222:113215.

[5] Rahimi MJ, Hamedi MH, Amidpour M. Thermodynamic and economic evaluation of a novel configuration for sustainable production of power and freshwater based on biomass gasification. Energy Systems. 2019.

[6] Ghorbani B, Ebrahimi A, Ziabasharhagh M, Rahimi MJ. Biomass Gasification Process Integration with Stirling Engine, Solid Oxide Fuel Cell, and Multi-Effect Distillation. Journal of Thermal Analysis and Calorimetry. 2020.

[7] Maraver D, Uche J, Royo J. Assessment of high temperature organic Rankine cycle engine for polygeneration with MED desalination: A preliminary approach. Energy Conversion and Management. 2012;53:108-17.

[8] Calise F, Macaluso A, Piacentino A, Vanoli L. A novel hybrid polygeneration system supplying energy and desalinated water by renewable sources in Pantelleria Island. Energy. 2017;137:1086-106.

[9] Rahimi MJ, Hamedi MH, Amidpour M, Livani E. Technoeconomic Evaluation of a Gasification Plant: Modeling, Experiment and Software Development. Waste and Biomass Valorization. 2020:1-26.

[10] Rahimi M, Hamedi MH, Amidpour M. Thermodynamic simulation and economic modeling and optimization of a multi generation system partially fed with synthetic gas from gasification plant. Gas Processing Journal. 2017;5:49-68.

[11] Sayyaadi H, Ghorbani G. Conceptual design and optimization of a small-scale dual power-desalination system based on the Stirling prime-mover. Applied Energy. 2018;223:457-71.

[12] Salimi M, Amidpour M. Investigating the integration of desalination units into cogeneration systems utilizing R-curve tool. Desalination. 2017;419:49-59.

[13] Sadri S, Ameri M, Khoshkhoo RH. Multi-objective optimization of MED-TVC-RO hybrid desalination system based on the irreversibility concept. Desalination. 2017;402:97-108.

[14] Mokhtari H, Sepahvand M. Thermoeconomic and exergy analysis in using hybrid systems (GT+ MED+ RO) for desalination of brackish water in Persian Gulf. Desalination. 2016;399:1-15.

[15] Almutairi A, Pilidis P, Al-Mutawa N, Al-Weshahi M. Energetic and exergetic analysis of cogeneration power combined cycle and ME-TVC-MED water desalination plant: Part-1 operation and performance. Applied Thermal Engineering. 2016;103:77-91.

[16] Wu X, Hu Y, Wu L, Li H. Model and Design of Cogeneration System for Different Demands of Desalination Water,

Heat and Power Production. Chinese Journal of Chemical Engineering. 2014;22:330-8.
[17] Shakib SE, Amidpour M, Aghanajafi C. Simulation and optimization of multi effect desalination coupled to a gas turbine plant with HRSG consideration. Desalination. 2012;285:366-76.
[18] Ansari K, Sayyaadi H, Amidpour M. A comprehensive approach in optimization of a dual nuclear power and desalination system. Desalination. 2011;269:25-34.
[19] Ameri M, Mohammadi SS, Hosseini M, Seifi M. Effect of design parameters on multi-effect desalination system specifications. Desalination. 2009;245:266-83.
[20] Kamali RK, Abbassi A, Sadough Vanini SA, Saffar Avval M. Thermodynamic design and parametric study of MED-TVC. Desalination. 2008;222:596-604.
[21] Nisan S, Dardour S. Economic evaluation of nuclear desalination systems. Desalination. 2007;205:231-42.
[22] Agashichev SP, El-Nashar AM. Systemic approach for techno-economic evaluation of triple hybrid (RO, MSF and power generation) scheme including accounting of CO2 emission. Energy. 2005;30:1283-303.
[23] Al-Hengari S, El-Bousiffi M, El-Mudir W. Performance analysis of a MSF desalination unit. Desalination. 2005;182:73-85.
[24] Alasfour FN, Darwish MA, Bin Amer AO. Thermal analysis of ME—TVC+MEE desalination systems. Desalination. 2005;174:39-61.
[25] Kahraman N, Cengel YA. Exergy analysis of a MSF distillation plant. Energy Conversion and Management. 2005;46:2625-36.
[26] Bejan A, Tstsaronis G, Moran M. Thermal Design and Optimization: Wiley; 1996.
[27] Thermoflow (GTpro module). Thermoflow Inc.